

Forcing of the Arctic Oscillation by Eurasian Snow Cover

ROBERT J. ALLEN* AND CHARLES S. ZENDER

Department of Earth System Science, University of California, Irvine, Irvine, California

(Manuscript received 22 October 2010, in final form 9 May 2011)

ABSTRACT

Throughout much of the latter half of the twentieth century, the dominant mode of Northern Hemisphere (NH) extratropical wintertime circulation variability—the Arctic Oscillation (AO)—exhibited a positive trend, with decreasing high-latitude sea level pressure (SLP) and increasing midlatitude SLP. General circulation models (GCMs) show that this trend is related to several factors, including North Atlantic SSTs, greenhouse gas/ozone-induced stratospheric cooling, and warming of the Indo-Pacific warm pool. Over the last approximately two decades, however, the AO has been decreasing, with 2009/10 featuring the most negative AO since 1900. Observational and idealized modeling studies suggest that snow cover, particularly over Eurasia, may be important. An observed snow–AO mechanism also exists, involving the vertical propagation of a Rossby wave train into the stratosphere, which induces a negative AO response that couples to the troposphere. Similar to other GCMs, the authors show that transient simulations with the Community Atmosphere Model, version 3 (CAM3) yield a snow–AO relationship inconsistent with observations and dissimilar AO trends. However, Eurasian snow cover and its interannual variability are significantly underestimated. When the albedo effects of snow cover are prescribed in CAM3 (CAM PS) using satellite-based snow cover fraction data, a snow–AO relationship similar to observations develops. Furthermore, the late-twentieth-century increase in the AO, and particularly the recent decrease, is reproduced by CAM PS. The authors therefore conclude that snow cover has helped force the observed AO trends and that it may play an important role in future AO trends.

1. Introduction

The Arctic Oscillation (AO) (Thompson and Wallace 1998) and its regional manifestation, the North Atlantic Oscillation (NAO) (Wallace and Gutzler 1981), are associated with climate variability that affects much of North America and Eurasia (EA). This includes north–south shifts of zonal wind and storminess and large anomalies in surface temperature and precipitation. Although both appear to be fundamental, internal modes of the atmosphere, they may be modulated by external forcings (Shindell et al. 1999; Feldstein 2002; Gong et al. 2002). Several such external forcings have been identified, although no dominant mechanism has been clearly established.

Atmospheric general circulation model (AGCM) simulations have showed that much of the multiannual to multidecadal variability of the NAO, as well as the late-twentieth-century trend, is related to North Atlantic SSTs (Rodwell et al. 1999; Robertson et al. 2000). AGCMs have also showed that warming of tropical SSTs—in particular those in the equatorial Indian and western Pacific Oceans—has helped force the NAO trend (Hoerling et al. 2001; Hurrell et al. 2004). This is consistent with the coupled climate model experiments of Selten et al. (2004). Several studies also showed that increasing greenhouse gases (GHGs)—by strengthening the upper-troposphere/lower-stratosphere (UT/LS) meridional temperature gradient—force positive AO trends (Shindell et al. 1999; Fyfe et al. 1999; Osborn 2004; Miller et al. 2006). Changing concentrations of atmospheric aerosols may also have an impact on AO trends (Chung and Ramanathan 2003; Allen and Sherwood 2011), but this effect remains highly uncertain.

Significant observational evidence relates Eurasian snow cover to the AO, influencing its phase, strength, and interannual variability (Cohen and Entekhabi 1999; Saito and Cohen 2003; Cohen and Barlow 2005).

* Current affiliation: Scripps Institution of Oceanography, La Jolla, California.

Corresponding author address: Robert Allen, CASPO, Scripps Institution of Oceanography, 9500 Gilman Drive, La Jolla, CA 92093.
E-mail: rjallen@uci.edu

Observations also support a snow–AO mechanism, whereby anomalously high Eurasian snow cover in autumn results in an increase in upward stationary Rossby wave activity, which slows the stratospheric polar vortex and increases high-latitude geopotential heights. This anomaly then propagates downward through the troposphere, resulting in a negative AO-like response at the surface during winter (Saito et al. 2001; Cohen et al. 2007; Hardiman et al. 2008). Cohen et al. (2010) argued that the record low AO values of 2009/10 were the result of a rapid advance in Eurasian snow cover, as well as persistently extensive EA snow cover, which resulted in the unusual occurrence of two troposphere–stratosphere coupling events.

One study in particular concluded that fall Eurasian snow cover anomalies—and not the other aforementioned mechanisms—have likely forced the wintertime AO (Cohen and Barlow 2005). Over the last approximately two decades, EA snow cover is best matched with the AO in terms of both pattern and trend, with similar decadal swings in both and no mismatch where trends are present in the AO—but not in the mechanism. Similarly, Cohen et al. (2009) showed that late-winter NH cooling temperature trends over the last two decades are related to the negative AO and partially forced by increasing EA fall snow cover. Recently, Allen and Zender (2011) showed that interannual persistence of the snow–AO mechanism (particularly on the 2–3-yr time scale) is related to soil moisture anomalies and an evaporation–convection feedback, which sustains the snowmelt–soil moisture anomaly through the summer. Alternatively, Bojariu and Gimeno (2003) argued that NAO persistence comes from winter/spring NAO circulation anomalies influencing snow cover, which in turn affect the NAO in summer/fall.

GCM studies with freely varying snow are unable to reproduce the observed snow–AO relationship. This includes the correlation between fall EA snow anomalies and the winter AO (Cohen et al. 2005), as well as the correlation between fall EA snow anomalies and upward propagating wave activity (Hardiman et al. 2008). Model deficiencies in snow cover may be responsible, as most GCMs underestimate EA snow cover interannual variability (Hardiman et al. 2008) and trends (Flanner et al. 2009).

In this paper, we present the first transient GCM experiments that reproduce the observed snow–AO relationship. Similar to other GCMs with freely evolving snow, we show that the Community Atmosphere Model (CAM) snow–AO relationship and the corresponding AO trends are inconsistent with observations. However, the CAM Eurasian snow cover and its interannual variability are underestimated. Similar experiments with prescribed snow cover yield significant improvements, with AO trends similar to observations. This paper is organized as follows. Section 2 describes our experimental design and

snow prescription method. Results are presented in section 3, followed by a discussion and conclusions in section 4.

2. Methods

We use the Community Atmosphere Model, version 3 (Collins et al. 2004) at T42 resolution ($\sim 2.8^\circ \times 2.8^\circ$) with 26 vertical levels and a model top at 2.9 hPa. CAM is coupled to the Community Land Model (CLM), version 3 (Oleson et al. 2004), which combines realistic radiative, ecological, and hydrologic processes. This work builds upon our prior, more idealized snow–AO study (Allen and Zender 2010) in which a pair of 100 ensemble member CAM experiments was forced with prescribed high and low EA snow albedo over a single fall–winter. There, we found anomalous EA snow albedo produces significant surface/lower-tropospheric cooling and a wave activity pulse that propagates into the stratosphere, culminating in a negative phase AO-like surface response. Therefore, the primary mechanism by which anomalous snow cover affects high-latitude circulation is through diabatic cooling via enhanced albedo. Here, we extend those ideas and basic experimental design to more realistic climate simulations using two 10-ensemble-member transient integrations from 1972 to 2006. Both long-term ensembles use the following time-varying forcing as in Flanner et al. (2009): GHGs, ozone, sulfate, volcanic aerosols, black and organic carbon (radiatively active in the atmosphere only), sea ice, and SSTs. One 10-member set uses prognostic snow cover based on the CAM default snow cover fraction (SCF) parameterization. The other 10-member set is analogous, but snow is prescribed by incorporating its effects on surface albedo. At each model time step and NH grid point, the CAM prognostic SCF is replaced with that based on monthly NOAA satellite data (<http://climate.rutgers.edu/snowcover/index.php>), interpolated to daily values at T42 resolution. This observation-based SCF is then used by CAM to estimate surface albedo [see Allen and Zender (2010) for additional details].

In this paper, we use the vertical wave activity flux (WAF) to quantify the upward propagation of planetary waves (Plumb 1985) and polar cap ($\geq 60^\circ\text{N}$) geopotential height (Z_{PC}) as a representative measure of the AO. Trend significance is based on a Student's t test, accounting for the reduction in the number of degrees of freedom due to autocorrelation (Wilks 1995). For correlation coefficients r , the t value is calculated according to $r\sqrt{(n-2)(1-r^2)^{-1}}$, where n is the number of years. The effective time between independent samples is estimated from the autoregressive properties of both time series (Livezey 1999). Field significance of correlations is evaluated by calculating the percentage of the given area with locally significant tests and comparing this test

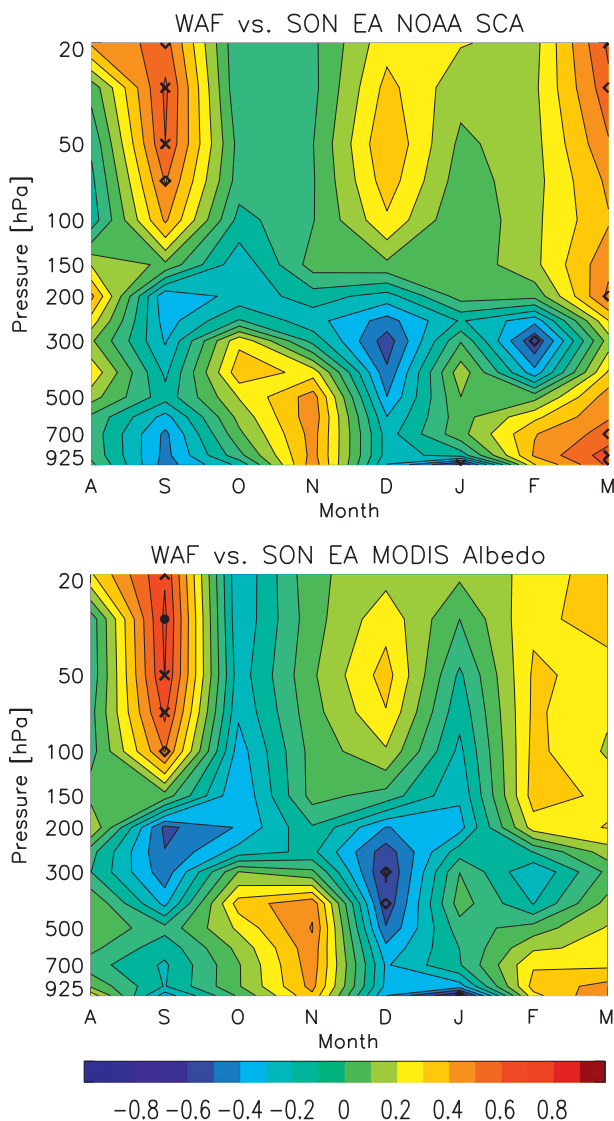


FIG. 1. Correlations for 2000–10 between August–March NCEP–NCAR WAF 40°–80°N and (top) SON EA NOAA SCA and (bottom) SON EA MODIS albedo. Symbols represent significance (based on a Student's t test accounting for autocorrelation) at the 90% (diamond), 95% (cross), and 99% (dot) confidence levels.

statistic to a null distribution based on a moving-blocks bootstrap (Chen 1982; Wilks 1995; Livezey 1999). For most correlations, the area percentage of locally significant points is larger than the corresponding 95% percentile of the null distribution and is not discussed further.

3. Results

a. EA snow cover versus albedo

As previously mentioned, Allen and Zender (2010) found that the primary mechanism by which anomalous

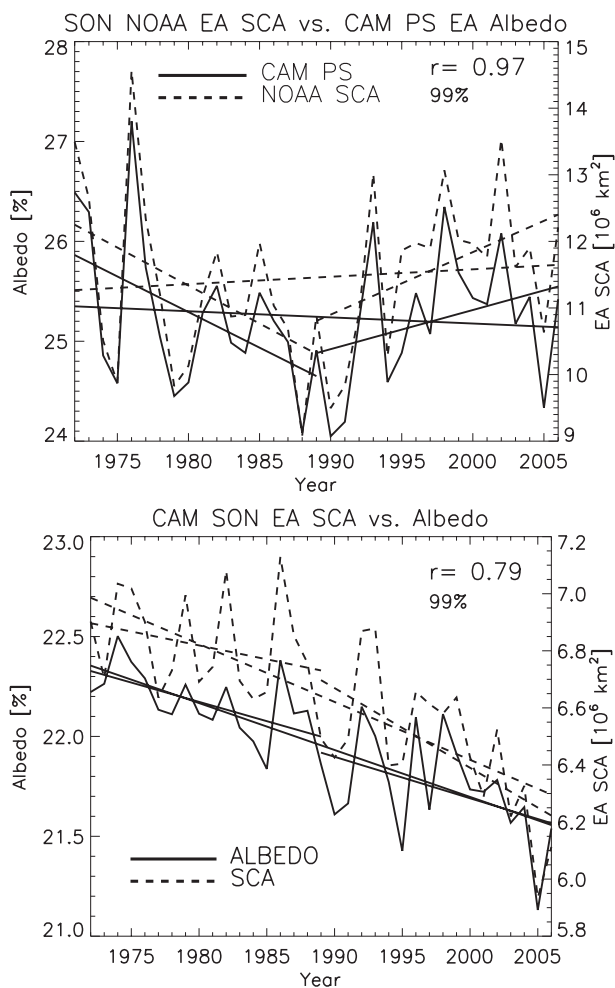


FIG. 2. (top) SON Eurasian SCA for 1972–2006 based on NOAA satellite observations and the corresponding CAM Eurasian albedo with prescribed snow (CAM PS) and (bottom) SON EA SCA and albedo based on CAM with prognostic snow. For the top panel, trends in both subperiods (1972–89 and 1989–2006) are significant at the 90% confidence level; a detrended correlation coefficient is included in each panel.

Eurasian snow cover affects high-latitude circulation is through the albedo effect, which results in enhanced surface cooling and increased vertically propagating wave activity. The close correspondence between snow cover area (SCA) and surface albedo is further supported by satellite observations. Albedo data from 2000 to 2010 comes from the 16-day 0.05° *Terra* and *Aqua* Moderate Resolution Imaging Spectroradiometer (MODIS) combined albedo product on the Climatological Modeling Grid (MCD43C) (Schaaf et al. 2002). Over Eurasia during September–November (SON), the detrended correlation between the MODIS white-sky shortwave (0.3–5.0 μm) albedo and NOAA SCA is 0.85. Furthermore, the corresponding correlation between MODIS white-sky

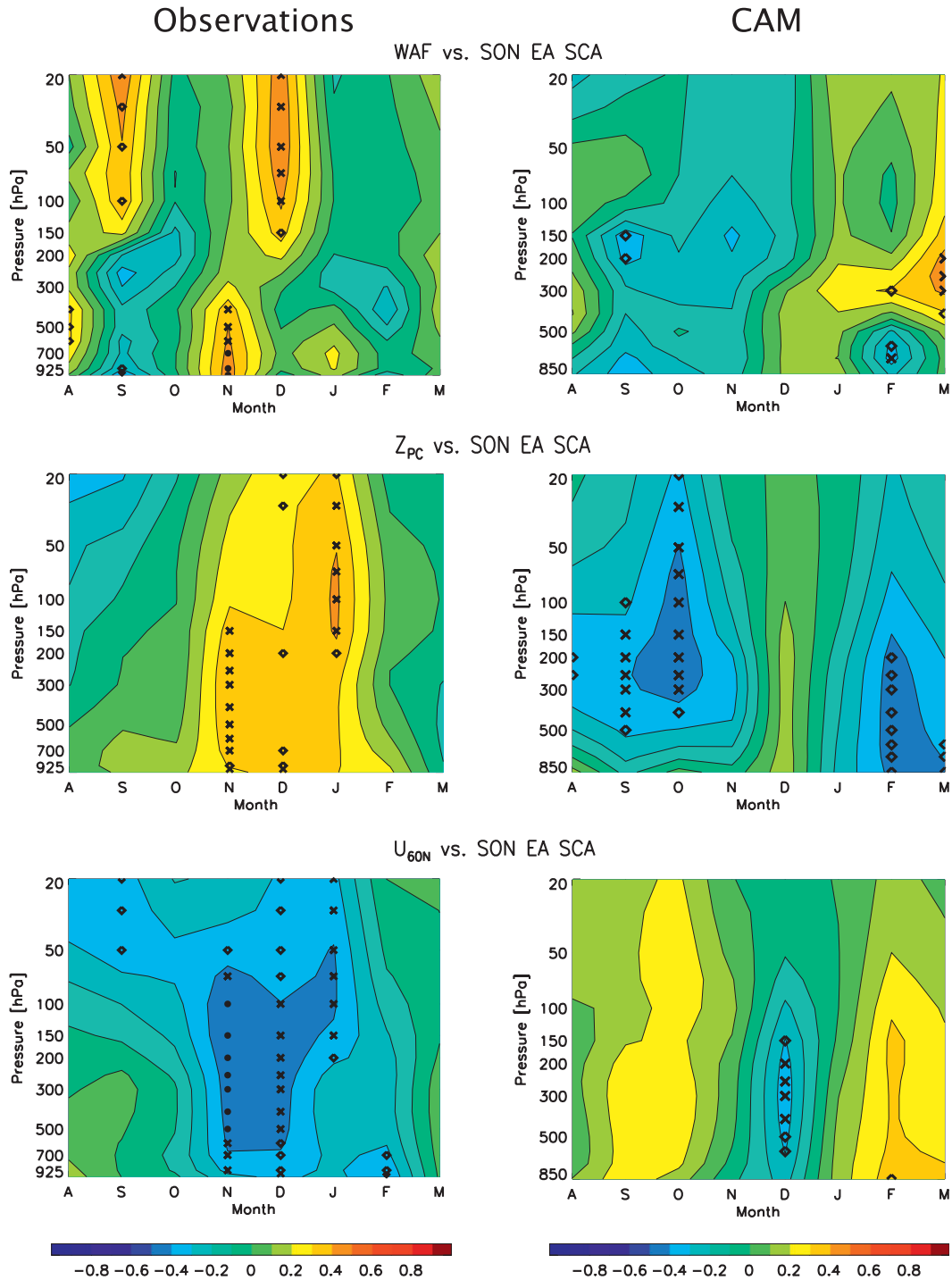


FIG. 3. Correlations for 1972–2006 between SON Eurasian SCA and August–March (top) WAF 40°–80°N, (middle) Z_{PC} and (bottom) U_{60N} for (left) observations and (right) CAM with prognostic snow. Symbols represent significance as in Fig. 1. Observations consist of NCEP–NCAR reanalysis data for atmospheric variables and NOAA satellite data for snow cover. Data are detrended before correlation estimation (similar results exist without detrending).

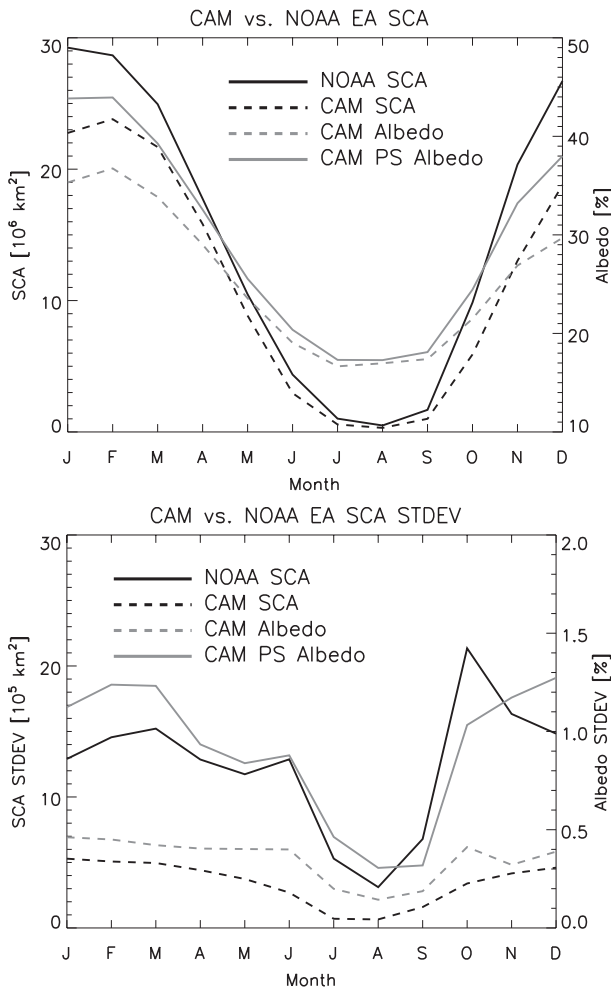


FIG. 4. Monthly (top) Eurasian SCA and (bottom) its standard deviation for NOAA satellite observations and CAM. Also included are the analogous CAM and CAM PS values based on albedo.

shortwave albedo and MODIS SCA is 0.98. Similar results are obtained for MODIS black-sky shortwave albedo, and both black- and white-sky band 4 (0.545–0.565 μm) albedos. All quantities (albedo and SCA) possess small, decreasing trends over the 11-y period. These observational results further support the close relationship between EA SON SCA and surface albedo, and justify our experimental design of prescribing snow via albedo.

Figure 1 shows the 2000/10 monthly (August–March) correlations between WAF 40° and 80°N and SON EA NOAA SCA, and separately for SON EA MODIS (white-sky shortwave) albedo. Consistent with the snow–AO relationship, positive Eurasian fall snow anomalies are associated with an increase in tropospheric WAF in November and stratospheric WAF in December (the long-term relationship is stronger and is discussed in the subsequent section). A nearly identical WAF relationship also

exists for EA SON MODIS albedo. This analysis shows that the albedo effect is the primary mechanism by which enhanced eurasian SON snow cover increases Rossby wave activity, the first step in the snow–AO relationship.

Figure 2 shows the close correspondence between the NOAA SON EA SCA time series and the corresponding surface albedo time series from CAM with prescribed snow (CAM PS). Similar interannual variations exist with a detrended correlation coefficient of 0.97. Similar trends also exist, particularly for the three periods considered: the overall period from 1972 to 2006, as well as the two subperiods obtained by dividing this in half, 1972–89 and 1989–2006. Figure 2 also shows the close correspondence between CAM SON EA (prognostic) SCA and albedo, with a detrended correlation coefficient of 0.79.

b. CAM snow–AO relationship

Figure 3 shows the 1972–2006 ensemble-mean monthly (August–March) CAM correlations between September–October (SON) EA SCA and WAF 40°–80°N, as well as the correlations between SON EA SCA and Z_{PC} and zonal wind at 60°N (U_{60N}). Consistent with the close correspondence between CAM SCA and albedo (Fig. 2), similar results are obtained when CAM SON EA albedo, instead of SCA, is used (not shown). Also included in Fig. 3 are the corresponding plots based on the National Centers for Environmental Prediction–National Center for Atmospheric Research (NCEP–NCAR) reanalysis using NOAA SCA (the NOAA SCA–WAF plot is similar to that in Fig. 1 but based on 1972–2006). Observations show that positive Eurasian fall snow anomalies are associated with an increase in tropospheric (stratospheric) WAF in November (December), as well as an increase in wintertime Z_{PC} and a decrease in U_{60N} , both consistent with the negative AO phase. Similar to most GCMs (Hardiman et al. 2008), CAM is unable to reproduce the observed snow–AO relationship. CAM correlations between SON EA SCA and WAF bear little resemblance to reanalysis; during October–December (OND), correlations are mostly negative, opposite observations. Similarly, the relation between SON EA SCA and both Z_{PC} and U_{60N} is generally opposite that based on observations, with significant negative and positive correlations, respectively, throughout fall and winter. The lone exception is in the troposphere during December when CAM shows significant negative U_{60N} and weak positive Z_{PC} correlations.

The snow–AO relationship provides a stringent test for GCMs; there are several reasons (e.g., Hardiman et al. 2008) why they may be unable to capture the snow–AO relationship. Figure 4 shows the ensemble-mean CAM monthly EA SCA and albedo, their standard deviation, and the corresponding SCA values based on NOAA satellite observations. Both SCA quantities are

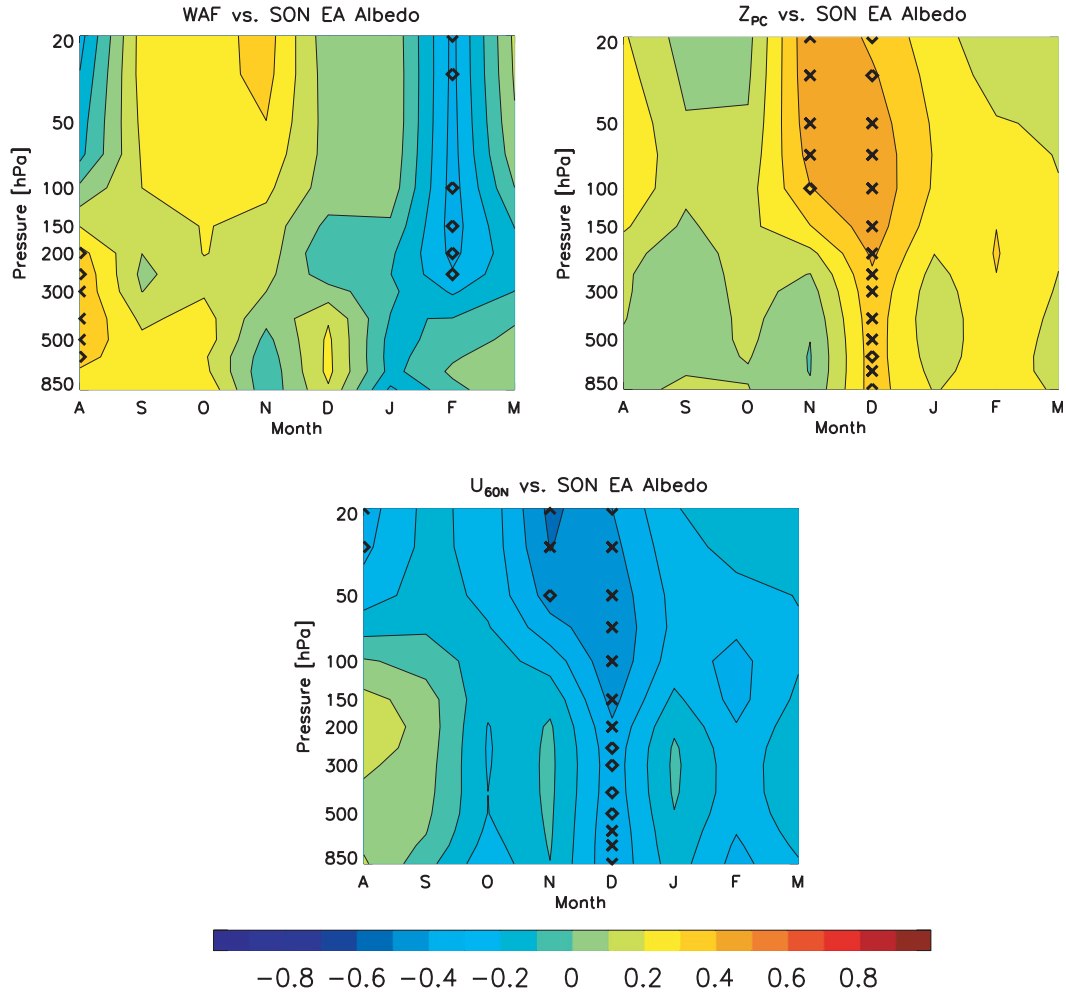


FIG. 5. As in Fig. 3, but based on CAM PS featuring prescribed snow. Correlations are based on SON EA albedo, as opposed to SCA.

underestimated by CAM, particularly during the important fall months, when October SCA is underestimated by 40% and its standard deviation is underestimated by 85%. This suggests that the CAM poor snow–AO simulation is partly due to its representation of snow cover. To test this hypothesis, analogous CAM experiments with prescribed snow were performed. Figure 4 shows that these experiments have much larger SCA interannual variability (as represented by albedo) that better resembles the observed climatology. Figure 4 also shows that the seasonal cycle and interannual variability of CAM albedo (with prognostic snow) is significantly less than that with CAM PS (with prescribed NOAA SCA). In October, Eurasian albedo is 21.5% in CAM, compared to 24.4% in CAM PS, an ~14% underestimation bias. The lack of correspondence between NOAA SCA and CAM PS albedo is due to the nonlinear relationship; the summer offset is due to the fact surface albedo

approaches the no-snow ground albedo, whereas SCA approaches zero.

c. CAM PS snow–AO relationship

Figure 5 shows that the snow–AO relationship with CAM PS better resembles observations. A positive correlation between WAF 40° and 80°N and SON albedo (i.e., SCA) exists in the fall, with tropospheric-to-stratospheric propagation. The correlation between SON albedo and Z_{PC} also better resembles observations, with positive correlations throughout November–February and the most significant correlations in December. Furthermore, the snow-induced decrease in zonal wind at 60°N also better resembles observations, with negative correlations throughout most of the winter and maximum values in December.

Although the CAM PS snow–AO relationship is significantly improved, the response is more diffuse and

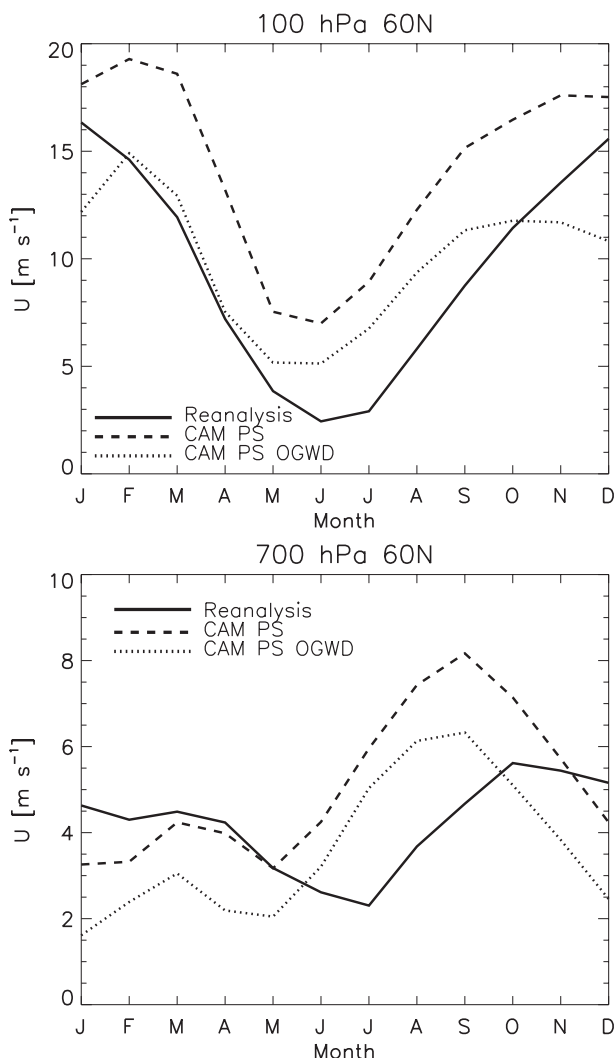


FIG. 6. Climatological (top) 100-hPa and (bottom) 700-hPa zonal wind U_{60N} for the NCEP–NCAR reanalysis, CAM PS, and CAM PS OGWD.

premature. For example, the observed snow–wave activity flux relationship (Fig. 3) exhibits significant positive correlations confined to November (in the troposphere) and December (in the stratosphere). CAM PS WAF correlations, however, are spread throughout the fall–early winter and occur approximately one month too early with maximum stratospheric correlations in November. Similarly, maximum Z_{PC} correlations exist in December, as opposed to January. Although sampling effects may explain some of this discrepancy, CAM overestimates the zonal mean flow through which WAF propagates, which could lead to the premature snow–AO response. Studies have shown a link between the strength of the winds in the mid-to-high-latitude upper troposphere/lower stratosphere (UT/LS) and the tropospheric annular mode response (e.g., Scaife

et al. 2005; Sigmond et al. 2008). Figure 6 shows that relative to the NCEP–NCAR reanalysis, CAM PS (and CAM, not shown) climatological 100-hPa zonal winds (U) at 60°N are $\sim 50\%$ too large during most months but particularly during boreal autumn. Thus, CAM PS SON UT/LS U is approximately equal to the NCEP–NCAR reanalysis OND U , indicating that the CAM monthly zonal wind climatology is shifted approximately one month earlier. Note that a similar bias exists in the troposphere (e.g., 700 hPa), particularly for summer through early fall.

The impact of this bias was tested by modifying the CAM orographic gravity wave drag (OGWD) parameterization, which accounts for the dissipation effects of unresolved gravity waves on stratospheric mean flow and controls the strength of the zonal wind in the mid to high-latitude lower stratosphere. Ten additional independent realizations of CAM PS with quadrupled OGWD efficiency (from the default value of 0.125 to 0.5) were conducted. Figure 6 shows that CAM PS OGWD has a much smaller SON U bias. Moreover, Fig. 7 shows that the OGWD modification delays the timing of the SON EA snow–WAF relationship with significant positive tropospheric correlations during December, followed by weak ($<90\%$ significant), but positive, stratospheric correlations in January. This supports the hypothesis that the premature snow–AO relationship with CAM PS is related to the fast wind bias. Note, however, the OGWD modification yields a snow–AO relationship that differs from CAM PS in several aspects. The weaker WAF correlations in the stratosphere may be due to the December and January winds being reduced too much (Fig. 6), leading to tropospheric trapping of the Rossby wave pulse. The significant negative correlations in November are related to destructive wave interference (Smith et al. 2010; Allen and Zender 2010) between the WAF response (the covariance between normalized SON albedo and monthly WAF at 60°N) and the monthly long-term mean WAF at 60°N. The corresponding pressure-weighted correlation is -0.47 in November, indicating that the Rossby wave response is relatively out of phase with the corresponding background stationary wave. In contrast, the corresponding correlation is 0.39 in December, indicating that the response is relatively in phase with the climatological wave. A similar set of CAM PS experiments with doubled—as opposed to quadrupled—OGWD efficiency did not remove as much of the U bias, nor did it improve the timing of the snow–AO relationship (not shown).

Consistent with the delayed snow–WAF relationship, Fig. 7 shows that the CAM PS OGWD SON EA albedo– Z_{PC} and U_{60N} relationships are also both delayed, with stratospheric correlations peaking in February. However, they are significantly weaker than the corresponding

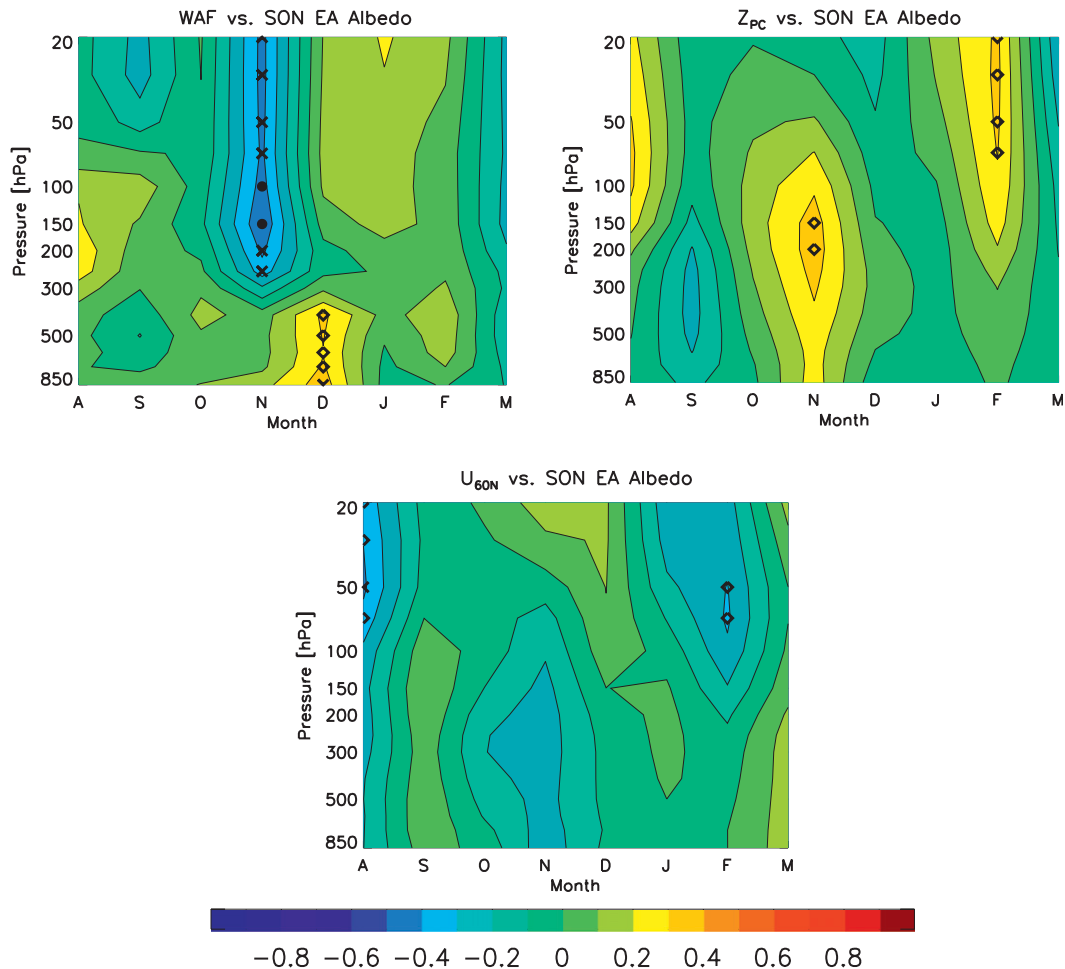


FIG. 7. As in Fig. 5, but based on CAM PS OGWD featuring prescribed snow with increased orographic wave drag.

CAM PS correlations (Fig. 5) and are confined to the stratosphere, due to reduced stratosphere–troposphere coupling (to be discussed below). The positive Z_{PC} tropospheric correlations in November are related to a corresponding increase in the meridional component of WAF (not shown). This is associated with enhanced poleward tropospheric wave activity, resulting in an equatorward momentum flux and deceleration of the zonal winds near 60°N and an increase in Z_{PC} .

Figure 8 quantifies the stratosphere–troposphere coupling in terms of the correlation between the December–February (DJF) AO (based on the leading principal component of sea level pressure poleward of 20°N) and August–March Z_{PC} . The NCEP–NCAR reanalysis shows statistically significant correlations between DJF sea level pressure and geopotential heights in both the stratosphere and troposphere from November through February. This strong coupling between the stratosphere and troposphere also exists with CAM and CAM PS (excluding November

for CAM). With CAM PS OGWD, however, the stratosphere–troposphere coupling is weaker. Stratospheric correlations are generally not significant; during February the relationship reverses. Although increasing the OGWD efficiency reduces the CAM fast wind bias and delays the timing of the snow–AO relationship, it also reduces the stratosphere–troposphere coupling. This results in reduced propagation of the snow-induced Z_{PC} and U_{60N} anomaly from the stratosphere to the troposphere, and a weaker snow–AO relationship.

d. Snow–AO trends

Figure 9 shows the time series of the Eurasian October SCA/albedo (multiplied by -1) and the DJF surface AO for CAM and CAM PS (plots end in 2005 since CAM integrations do not include January–February of 2007). Consistent with the aforementioned analysis, CAM shows a weak snow–AO relationship of the wrong sign, with an interannual correlation r of -0.13 . Correlating CAM

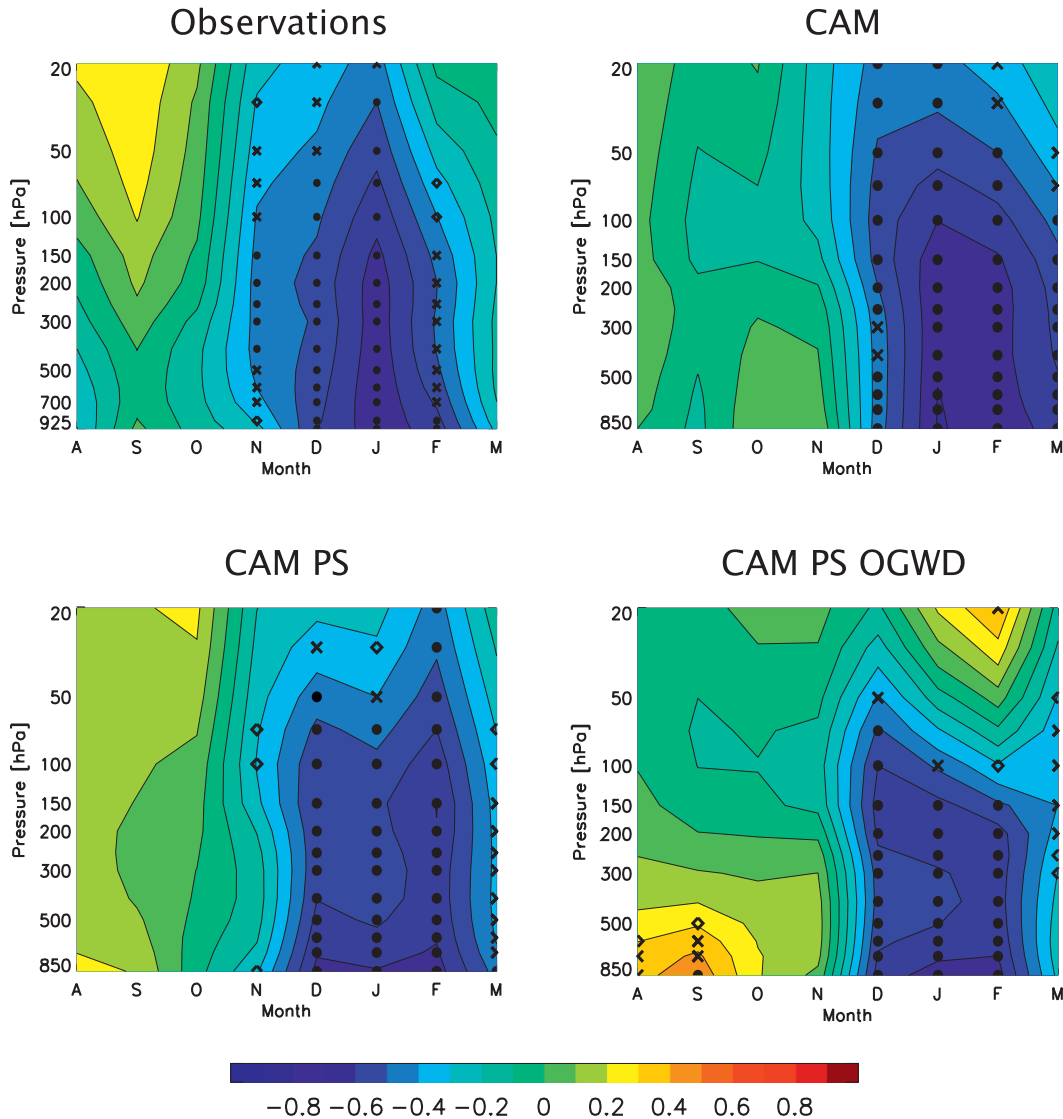


FIG. 8. 1972–2006 correlations between the DJF AO and August–March Z_{PC} for observations (NCEP–NCAR reanalysis) and all three CAM experiments. Symbols represent significance as in Fig. 3.

October albedo (instead of SCA) with the DJF AO results in a similar weak correlation of -0.12 . For CAM PS, however, the corresponding correlation is 0.32 , significant at the 90% confidence level. This is similar to, but smaller than, that based on the NCEP–NCAR reanalysis for which $r = 0.49$, 99% significant. A similar CAM PS relationship also exists for other seasons—the correlation between October albedo is 0.27 for the January–March (JFM) AO and 0.31 for the December–March (DJFM) AO. In agreement with the observed snow–AO relationship, somewhat weaker CAM PS correlations exist for EA SON albedo and the DJF ($r = 0.23$), JFM ($r = 0.23$), and DJFM AO ($r = 0.26$). The CAM PS AO also exhibits similar interannual variations as the observed

AO with a correlation of 0.29 during DJF, 90% significant (-0.03 for CAM).

The CAM PS—with an improved snow–AO relationship—also yields similar trends in the AO and EA October albedo. All three periods show the expected behavior, with decreasing albedo and increasing AO trends during the first half, increasing albedo and decreasing AO trends during the second half, and negligible trends over the entire period. Moreover, CAM PS AO trends are similar to those based on reanalysis. This is unlike the corresponding CAM trends—for the entire period, as well as for the second half—when the AO trends are negligible, despite decreasing SCA. These results are generally similar if the entire period is not subdivided evenly (e.g.,

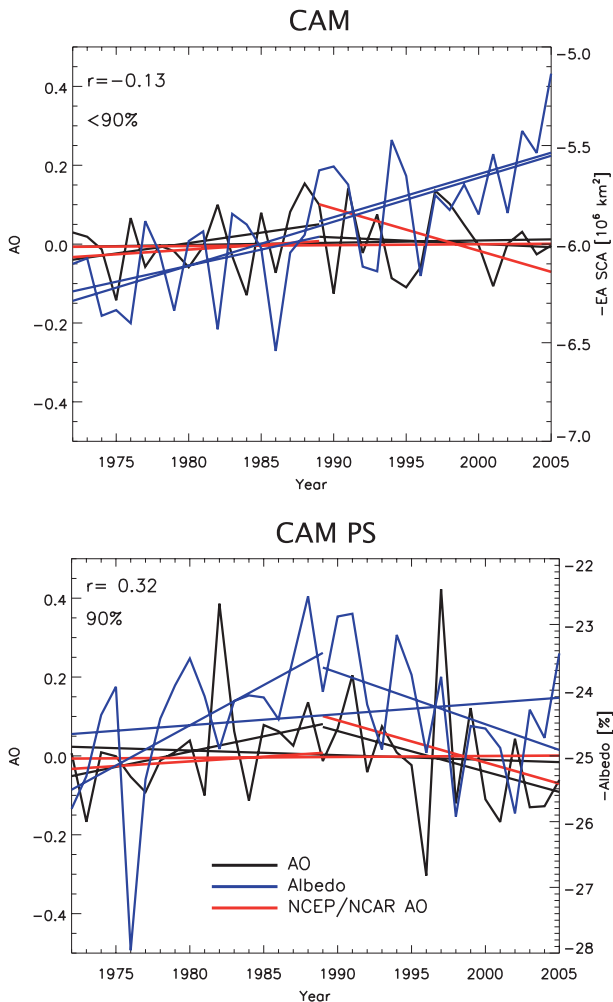


FIG. 9. 1972–2005 DJF AO and October EA SCA/albedo (multiplied by -1) for (top) CAM and (bottom) CAM PS. Also included are the corresponding linear trends for three periods: 1972–2005, 1972–89, and 1989–2005. Red lines correspond to the NCEP–NCAR AO trend. Detrended CAM SCA/albedo vs AO correlations for the entire time period are also included in the upper-left corner.

1972–90 and 1990–2005) or if other fall/winter months are chosen. This result suggests that Eurasian fall snow cover has helped force observed winter AO trends, particularly over the last two decades.

This ability of EA snow to force AO trends is further supported by an additional 10-member set of 35-yr CAM PS experiments but with EA fall snow cover—ranked from lowest to highest (i.e., year 1 is forced with the lowest EA SON albedo, year 2 with the second lowest, . . . , year 35 with the largest)—the only imposed forcing (climatological SSTs are used). To maintain fall–winter EA snow continuity, snow forcing in these experiments (CAM PSR) is based on an August–July calendar year. Figure 10 shows the resulting EA October albedo trend is

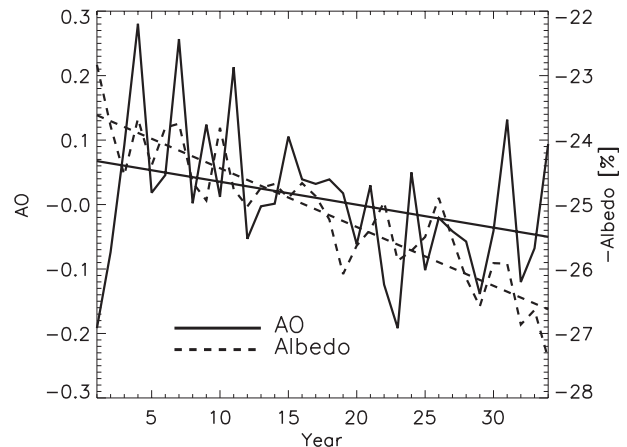


FIG. 10. As in Fig. 9, but based on CAM PSR, forced with prescribed snow only, ranked from lowest EA SON SCA to highest.

increasing and 99% significant (by design). The resulting DJF AO trend is decreasing and 90% significant. Similar negative trends also exist for the DJFM and JFM AO, which are 95% and 90% significant, respectively. Although less than 90% significant, the AO trend in individual months—including December, January, February, and March—are also all negative. This is consistent with the snow–AO relationship and the ability of Eurasian snow cover to force trends in the dominant mode of extratropical NH atmospheric variability.

4. Discussion and conclusions

Significant observational evidence exists relating Eurasian autumn snow cover to the subsequent winter's Arctic Oscillation (Cohen and Entekhabi 1999; Saito and Cohen 2003; Cohen and Barlow 2005). Observations also support a snow–AO mechanism, whereby anomalously high EA snow cover amplifies preexisting vertical wave activity that propagates into the stratosphere, producing a negative AO response that couples with the troposphere (Saito et al. 2001; Cohen et al. 2007; Hardiman et al. 2008). Most GCMs, however, are unable to simulate the observed snow–AO relationship (Cohen et al. 2005; Hardiman et al. 2008). We find that CAM3 similarly yields a poor snow–AO relationship, often of the wrong sign, with AO trends that differ from observations. However, EA snow cover and its interannual variability are significantly underestimated. When the albedo effects of snow cover are prescribed in CAM3 (CAM PS) using satellite-based snow cover fraction data, a snow–AO relationship similar to observations exists. Furthermore, the late-twentieth-century increase in the AO, and particularly the recent decrease, is reproduced by CAM PS. Although the CAM PS snow–AO relationship is significantly improved, the response is more diffuse and premature than

observations, with the CAM PS snow-induced wave activity flux pulse and increase in Z_{PC} occurring approximately one month too early. Further efforts to improve model simulation of the AO are therefore warranted, particularly model representation of snow cover.

As previously mentioned, the Arctic Oscillation is expected to exhibit a positive trend through the twenty-first century owing to increasing GHG concentrations (Shindell et al. 1999; Miller et al. 2006; Gillett et al. 2003). GHGs, however, will also contribute—and have contributed (Gillett et al. 2008)—to Arctic warming. Diminishing late-summer sea ice extent has been implicated as the leading cause, particularly for fall/winter near-surface warming (Screen and Simmonds 2010). Sea ice reductions may increase Arctic water vapor, which is consistent with the ECMWF interim reanalysis (ERA-Interim) during summer/early fall (Screen and Simmonds 2010). This may lead to more snow, which, by the snow–AO mechanism, favors a negative wintertime Arctic Oscillation. Idealized GCM experiments with prescribed sea ice reductions suggest such a link may exist, with increased Arctic water vapor (Higgins and Cassano 2009), precipitation, and Siberian snow depth (Deser et al. 2010). These experiments also generally yield a negative NAO (Magnusdottir et al. 2004), but minimal AO (Deser et al. 2010), response. Again, however, GCMs are unable to simulate the snow–AO relationship with freely evolving snow. If EA fall snow cover increases in a warmer world, our results suggest that the GHG-induced positive AO trend of the twenty-first century may be mitigated. Future research will attempt to quantitatively investigate such questions.

Acknowledgments. This study was funded by NSF ARC-0714088 and NASA NNX07AR23G, UC Irvine. We thank Mark Flanner for providing the prognostic BC/OC CAM3 code modifications, and for the time-varying aerosol forcing data sets. We also thank Xianwei Wang for providing processed MODIS albedo data and for additional assistance. Finally, we thank Judah Cohen and two anonymous reviewers for their insightful comments that significantly improved this manuscript.

REFERENCES

- Allen, R. J., and C. S. Zender, 2010: Effects of continental-scale snow albedo anomalies on the wintertime Arctic Oscillation. *J. Geophys. Res.*, **115**, D23105, doi:10.1029/2010JD014490.
- , and S. C. Sherwood, 2011: The impact of natural versus anthropogenic aerosols on atmospheric circulation in the Community Atmosphere Model. *Climate Dyn.*, **36**, 1959–1978, doi:10.1007/s00382-010-0898-8.
- , and C. S. Zender, 2011: The role of eastern Siberian snow and soil moisture anomalies in quasi-biennial persistence of the Arctic and North Atlantic Oscillations. *J. Geophys. Res.*, **116**, D16125, doi:10.1029/2010JD015311.
- Bojariu, R., and L. Gimeno, 2003: The role of snow cover fluctuations in multiannual NAO persistence. *Geophys. Res. Lett.*, **30**, 1156, doi:10.1029/2002GL015651.
- Chen, W. Y., 1982: Fluctuations in Northern Hemisphere 700 mb height field associated with the Southern Oscillation. *Mon. Wea. Rev.*, **110**, 808–823.
- Chung, C. E., and V. Ramanathan, 2003: South Asian haze forcing: Remote impacts with implications to ENSO and AO. *J. Climate*, **16**, 1791–1806.
- Cohen, J., and D. Entekhabi, 1999: Eurasian snow cover variability and Northern Hemisphere climate predictability. *Geophys. Res. Lett.*, **26**, 345–348.
- , and M. Barlow, 2005: The NAO, the AO, and global warming: How closely related? *J. Climate*, **18**, 4498–4513.
- , A. Frei, and R. D. Rosen, 2005: The role of boundary conditions in AMIP-2 simulations of the NAO. *J. Climate*, **18**, 973–981.
- , M. Barlow, P. J. Kushner, and K. Saito, 2007: Stratosphere–troposphere coupling and links with Eurasian land surface variability. *J. Climate*, **20**, 5335–5343.
- , —, and K. Saito, 2009: Decadal fluctuations in planetary wave forcing modulate global warming in late boreal winter. *J. Climate*, **22**, 4418–4426.
- , J. Foster, M. Barlow, K. Saito, and J. Jones, 2010: Winter 2009–2010: A case study of an extreme Arctic Oscillation event. *Geophys. Res. Lett.*, **37**, L17707, doi:10.1029/2010GL044256.
- Collins, W. D., and Coauthors, 2004: Description of the NCAR Community Atmosphere Model (CAM 3.0). NCAR Tech. Note NCAR/TN-464+STR, 226 pp.
- Deser, C., R. Tomas, M. Alexander, and D. Lawrence, 2010: The seasonal atmospheric response to projected Arctic sea ice loss in the late twenty-first century. *J. Climate*, **23**, 333–351.
- Feldstein, S. B., 2002: The recent trend and variance increase of the annular mode. *J. Climate*, **15**, 88–94.
- Flanner, M. G., C. S. Zender, P. G. Hess, N. M. Mahowald, T. H. Painter, V. Ramanathan, and P. J. Rasch, 2009: Springtime warming and reduced snow cover from carbonaceous particles. *Atmos. Chem. Phys.*, **9**, 2481–2497.
- Fyfe, J. C., G. J. Boer, and G. M. Flato, 1999: The Arctic and Antarctic Oscillations and their projected changes under global warming. *Geophys. Res. Lett.*, **26**, 1601–1604.
- Gillett, N. P., F. W. Zwiers, A. J. Weaver, and P. A. Stott, 2003: Detection of human influence on sea-level pressure. *Nature*, **422**, 292–294.
- , D. A. Stone, P. A. Stott, T. Nozawa, A. Y. Karpechko, G. C. Hegerl, M. F. Wehner, and P. D. Jones, 2008: Attribution of polar warming to human influence. *Nat. Geosci.*, **1**, 750–754.
- Gong, G., D. Entekhabi, and J. Cohen, 2002: A large-ensemble model study of the wintertime AO–NAO and the role of interannual snow perturbations. *J. Climate*, **15**, 3488–3499.
- Hardiman, S. C., P. J. Kushner, and J. Cohen, 2008: Investigating the ability of general circulation models to capture the effects of Eurasian snow cover on winter climate. *J. Geophys. Res.*, **113**, D21123, doi:10.1029/2008JD010623.
- Higgins, M. E., and J. J. Cassano, 2009: Impacts of reduced sea ice on winter Arctic atmospheric circulation, precipitation, and temperature. *J. Geophys. Res.*, **114**, D16107, doi:10.1029/2009JD011884.
- Hoerling, M., J. W. Hurrell, and T. Xu, 2001: Tropical origins for recent North Atlantic climate change. *Science*, **292**, 90–92.
- Hurrell, J. W., M. P. Hoerling, A. S. Phillips, and T. Xu, 2004: Twentieth century North Atlantic climate change. Part I: Assessing determinism. *Climate Dyn.*, **23**, 371–389.

- Livezey, R. E., 1999: Field intercomparison. *Analysis of Climate Variability: Applications of Statistical Techniques*, H. von Storch and A. Navarra, Eds., Springer, 161–178.
- Magnusdottir, G., C. Deser, and R. Saravanan, 2004: The effects of North Atlantic SST and sea ice anomalies on the winter circulation in CCM3. Part I: Main features and storm-track characteristics of the response. *J. Climate*, **17**, 857–876.
- Miller, R. L., G. A. Schmidt, and D. T. Shindell, 2006: Forced annual variations in the 20th century Intergovernmental Panel on Climate Change Fourth Assessment Report models. *J. Geophys. Res.*, **111**, D18101, doi:10.1029/2005JD006323.
- Oleson, K. W., and Coauthors, 2004: Technical description of the Community Land Model (CLM). NCAR Tech. Note NCAR/TN-461+STR, 174 pp.
- Osborn, T. J., 2004: Simulating the winter North Atlantic Oscillation: The roles of internal variability and greenhouse gas forcing. *Climate Dyn.*, **22**, 605–623.
- Plumb, R. A., 1985: On the three-dimensional propagation of stationary waves. *J. Atmos. Sci.*, **42**, 217–229.
- Robertson, A. W., C. R. Mechoso, and Y.-J. Kim, 2000: The influence of Atlantic sea surface temperature anomalies on the North Atlantic Oscillation. *J. Climate*, **13**, 122–138.
- Rodwell, M. J., D. P. Rowell, and C. K. Folland, 1999: Oceanic forcing of the wintertime North Atlantic Oscillation and European climate. *Nature*, **398**, 320–323.
- Saito, K., and J. Cohen, 2003: The potential role of snow cover in forcing interannual variability of the major Northern Hemisphere mode. *Geophys. Res. Lett.*, **30**, 1302, doi:10.1029/2002GL016341.
- , —, and D. Entekhabi, 2001: Evolution of atmospheric response to early-season Eurasian snow cover anomalies. *Mon. Wea. Rev.*, **129**, 2746–2760.
- Scaife, A. J., J. R. Knight, G. K. Vallis, and C. K. Folland, 2005: A stratospheric influence on the winter NAO and North Atlantic surface climate. *Geophys. Res. Lett.*, **32**, L18715, doi:10.1029/2005GL023226.
- Schaaf, C., and Coauthors, 2002: First operational BRDF, albedo nadir reflectance products from MODIS. *Remote Sens. Environ.*, **83**, 135–148.
- Screen, J. A., and I. Simmonds, 2010: The central role of diminishing sea ice in recent Arctic temperature amplification. *Nature*, **464**, 1334–1337.
- Selten, F. M., G. W. Branstator, H. A. Dijkstra, and M. Kliphuis, 2004: Tropical origins for recent and future Northern Hemisphere climate change. *Geophys. Res. Lett.*, **31**, L21205, doi:10.1029/2004GL020739.
- Shindell, D. T., R. L. Miller, G. A. Schmidt, and L. Pandolfo, 1999: Simulation of recent northern winter climate trends by greenhouse-gas forcing. *Nature*, **399**, 452–455.
- Sigmond, M., J. F. Scinocca, and P. J. Kushner, 2008: Impact of the stratosphere on tropospheric climate change. *Geophys. Res. Lett.*, **35**, L12706, doi:10.1029/2008GL033573.
- Smith, K. L., C. G. Fletcher, and P. J. Kushner, 2010: The role of linear interference in the annular mode response to extratropical surface forcing. *J. Climate*, **23**, 6036–6050.
- Thompson, D. W. J., and J. M. Wallace, 1998: The Arctic Oscillation signature in the wintertime geopotential height and temperature fields. *Geophys. Res. Lett.*, **25**, 1297–1300.
- Wallace, J. M., and D. S. Gutzler, 1981: Teleconnections in the geopotential height field during the Northern Hemisphere winter. *Mon. Wea. Rev.*, **109**, 784–812.
- Wilks, D. S., 1995: *Statistical Methods in the Atmospheric Sciences: An Introduction*. International Geophysics Series, Vol. 59, Academic Press, 467 pp.